Electrodeposition of Mesoporous Semimetal and Magnetic Metal Films from Lyotropic Liquid Crystalline Phases

Hongmei Luo,[†] Li Sun,[‡] Yunfeng Lu,[§] and Yushan Yan*,[†]

Department of Chemical and Environmental Engineering, University of California, Riverside, California 92521, Department of Mechanical Engineering, University of Houston, Houston, Texas 77057, and Department of Chemical and Biomolecular Engineering, Tulane University, New Orleans, Louisiana 70118

Received December 16, 2003. In Final Form: August 17, 2004

Mesoporous semimetal bismuth film and magnetic metal nickel and cobalt thin films have been electrodeposited from hexagonal or lamellar structured lyotropic liquid crystalline phases with polyoxyethylene surfactant. The liquid crystalline templates are characterized by low-angle X-ray diffraction (XRD) and polarized-light optical microscopy (POM). The metal films are characterized by low-angle and wide-angle XRD, scanning electron microscopy (SEM), and transmission electron microscopy (TEM). The magnetic measurements on the mesoporous nickel and cobalt films are shown to have higher coercivity (H_c) than the nonporous polycrystalline films.

Introduction

Bismuth (Bi) is a semimetal with unusual thermal, electrical, and magnetic transport properties that result from its highly anisotropic Fermi surface, low carrier concentration, small effective carrier mass, and long carrier mean free path.[1−3] There has been a long-standing interest in Bi nanostructures for both fundamental understanding and device fabrication. A large magnetoresistance (MR) effect was observed in Bi single crystal, thin film, and nanowire grown by molecular beam epitaxy or electrodeposition.[2−8] Bi was also extensively investigated as a thermoelectric material. Nanoporous Bi film has been prepared by the metalorganic deposition (MOD) method via spin-coating of bismuth organic precursor solution followed by pyrolysis reaction, and it was demonstrated that porous Bi film lowers the thermal conductivity and enhances the thermoelectric figure of merit.[9,10] However, the MOD method leads to thin films with random pores, and the pore size is not easily controlled.

Lyotropic liquid crystalline phases of polyoxyethylene surfactants can be utilized as versatile nanoscale molds for the formation of highly ordered mesoporous materials. Using this approach, mesoporous platinum, tin, palladium, cobalt, nickel, selenium, and tellurium films with hexagonal pore structure have been electrodeposited.[11−20] We have produced metal, semiconductor, conductive polymer nanowires, and hollow silica fibers by the use of liquid crystalline phases as templates.[21−25] Here we report the first synthesis of mesoporous Bi film with lamellar structure via the liquid crystal templated electrodeposition route. The ability to electrodeposit Bi films with well-defined mesoporous structures is important for studying the unusual transport properties and the influence of porosity on thermoelectric properties. Using this method, we also produced mesoporous magnetic metal nickel (Ni) and cobalt (Co) films with hexagonal or lamellar structures and studied their magnetic properties in comparison with the nonporous films.

Experimental Section

Materials. Nonionic surfactants polyoxyethylene(10) cetyl ether (Brij56, $C_{16}EO_{10}$), polyoxyethylene(10) stearyl ether (Brij76,

* Corresponding author: phone 909-787-2068; Fax 909-787-5696; e-mail yushan.yan@ucr.edu.
[†] University of California, Riverside.
[‡] University of Houston.
[§] Tulane University.

(1) Smith, G. E.; Baraff, G. A.; Rowell, J. M. *Phys. Rev.* **1964**, *135*, A1118.
(2) Hoffman, C. A.; Meyer, J. R.; Bartoli, F. J.; Di Venere, A.; Yi, X. J.; Hou, C. L.; Wang, H. C.; Ketterson, J. B.; Wong, G. K. *Phys. Rev. B* **1993**, *48*, 11431.
(3) Yang, F. Y.; Liu, K.; Hong, K.; Reich, D. H.; Searson, P. C.; Chien, C. L. *Phys. Rev. Lett.* **1999**, *82*, 3328; *Science* **1999**, *284*, 1355.
(4) Alers, P. B.; Webber, R. T. *Phys. Rev.* **1953**, *91*, 1060.
(5) Mangez, J. H.; Issi, J.-P.; Heremens, J. *Phys. Rev. B* **1976**, *14*, 4381.
(6) Partin, D. L.; Heremans, J.; Morelli, D. T.; Thrush, C. M.; Olk, C. H.; Perry, T. A. *Phys. Rev. B* **1988**, *38*, 3818.
(7) Vereecken, P. M.; Sun, L.; Searson, P. C.; Tanase, M.; Reich, D. H.; Chien, C. L. *J. Appl. Phys.* **2000**, *88*, 6529.
(8) Liu, K.; Chien, C. L.; Searson, P. C.; Kui, Y. Z. *Appl. Phys. Lett.* **1998**, *73*, 1436.
(9) Song, D. W.; Shen, W.-N.; Zeng, T.; Liu, W.; Chen, G.; Dunn, B.; Moore, C. D.; Goorsky, M. S.; Radetic, T.; Gronsky, R. *Proc. ASME Heat Transfer Div.* **1999**, *364−1*, 345.
(10) Shen, W.-N.; Dunn, B.; Moore, C. D.; Goorsky, M. S.; Radetic, T.; Gronsky, R. *J. Mater. Chem.* **2000**, *10*, 657.
(11) Attard, G. S.; Bartlett, P. N.; Coleman, N. R. B.; Elliott, J. M.; Owen, J. R.; Wang, J. H. *Science* **1997**, *278*, 838.
(12) Goltner-Spickermann, C. *Top. Curr. Chem.* **2003**, *226*, 29.
(13) Elliott, J. M.; Attard, G. S.; Bartlett, P. N.; Coleman, N. R. B.; Merckel, D. A. S.; Owen, J. R. *Chem. Mater.* **1999**, *11*, 3602.
(14) Attard, G. S.; Elliott, J. M.; Bartlett, P. N.; Whitehead, A.; Owen, J. R. *Macromol. Symp.* **2000**, *156*, 179.
(15) Bartlett, P. N.; Gollas, B.; Guerin, S.; Marwan, J. *Phys. Chem. Chem. Phys.* **2002**, *4*, 3835.
(16) Bartlett, P. N.; Birkin, P. N.; Ghanem, M. A.; de Groot, P. A. J.; Sawicki, M. *J. Electrochem. Soc.* **2001**, *148*, C119.
(17) Nelson, P. A.; Elliott, J. M.; Attard, G. S.; Owen, J. R. *Chem. Mater.* **2002**, *14*, 524; *J. New Mater. Electrochem. Syst.* **2002**, *5*, 63.
(18) Zhukov, A. A.; Goncharov, A. V.; de Groot, P. A. J.; Bartlett, P. N.; Ghanem, M. A. *J. Appl. Phys.* **2003**, *93*, 7322.
(19) Nandhakumar, I.; Elliott, J. M.; Attard, G. S. *Chem. Mater.* **2001**, *13*, 3840.
(20) Gabriel, T.; Nandhakumar, I. S.; Attard, G. S. *Electrochem. Commun.* **2002**, *4*, 610.
(21) Huang, L. M.; Wang, H. T.; Wang, Z. B.; Mitra, A.; Bozhilov, K. N.; Yan, Y. S. *Adv. Mater.* **2002**, *14*, 61.
(22) Huang, L. M.; Wang, H. T.; Wang, Z. B.; Mitra, A.; Zhao, D. Y.; Yan, Y. S. *Chem. Mater.* **2002**, *14*, 876.
(23) Huang, L. M.; Wang, Z. B.; Wang, H. T.; Cheng, X. L.; Mitra, A.; Yan, Y. S. *J. Mater. Chem.* **2002**, *12*, 388.
(24) Huang, L. M.; Wang, H. T.; Hayashi, C. Y.; Tian, B. Z.; Zhao, D. Y.; Yan, Y. S. *J. Mater. Chem.* **2003**, *13*, 666.
(25) Luo, H. M.; Zhang, J. F.; Yan, Y. S. *Chem. Mater.* **2003**, *15*, 3769.

10.1021/la036367+ CCC: $27.50
Published on Web 10/08/2004

$C_{18}EO_{10}$), and polyoxyethylene(20) stearyl ether (Brij78, $C_{18}EO_{20}$) were purchased from Aldrich. Bismuth nitrate ($Bi(NO_3)_3$), potassium nitrate (KNO_3), L-tartaric acid ($HOOC(CHOH)_2COOH$), nitric acid (HNO_3), glycerol, nickel acetate ($NiAc_2$), cobalt acetate ($CoAc_2$), nickel chloride ($NiCl_2$), nickel sulfamate ($Ni(H_2NSO_3)_2$, cobalt sulfate ($CoSO_4 \cdot 7H_2O$), sodium acetate (NaAc), sodium chloride (NaCl), potassium acetate (KAc), boric acid (H_3BO_3), and Pt gauze were from Alfa Aesar. The Ag/AgCl (3 M NaCl) electrode was from Bioanalytical systems, Inc. Indium tin oxide (ITO)-coated glass plates (ITO thickness: 175 ± 25 nm; resistance: $6 \pm 2\ \Omega$) were from Delta Technology. Distilled water (DI water) was passed through a Barnstead system until its resistivity reached 17 MΩ·cm. All the chemicals were used as received.

Film Synthesis. The experiment was performed under ambient conditions in a standard three-electrode glass cell. Pt gauze was used as the anode. Ag/AgCl electrode was used as the reference electrode ($U_{eq} = 0.215$ V standard hydrogen electrode, SHE). The working electrode was a 50 nm thick gold film sputter deposited on a Si(100) wafer with a presputtered 2 nm chromium adhesion layer or ITO glass. The electrolyte used in the electrodeposition of mesoporous Bi films consisted of a 50 wt % Brij56 or Brij76 surfactant and a 50 wt % aqueous solution with composition of 0.15 M $Bi(NO_3)_3$, 1 M KNO_3, 0.33 M L-tartaric acid, 0.65 M HNO_3, and 10 vol % glycerol (pH of the aqueous solution was adjusted around 0.3−0.6 by using HNO_3). The electrolyte for mesoporous Ni or Co films consisted of a 60 wt % Brij56, Brij76, or Brij78 surfactants and a 40 wt % aqueous solution containing 0.2 M $NiAc_2$, 0.5 M NaAc, and 0.2 M H_3BO_3 or 0.08 M $NiCl_2$, 1.6 M $Ni(H_2NSO_3)_2$, and 0.3 M H_3BO_3, or 0.4 M $CoAc_2$, 0.51 M KAc, and 0.16 M H_3BO_3, or 0.9 M $CoSO_4$, 0.8 M H_3BO_3, and 0.02 M NaCl (pH is 3−5).[16,17,26] To prepare the liquid crystal electrolyte, surfactant was first heated to around 50−60 °C to be melted, and then the aqueous solution was added dropwise with stirring. A clear viscous liquid was obtained after 10 min. Electrodeposition was carried out using a Solartron 1287 potentiostat. Bi films were deposited potentiostatically at −0.3 V vs Ag/AgCl, and Ni and Co films were deposited at −1 V vs Ag/AgCl. After deposition, the film was rinsed in purified water and soaked in DI water for 2 days which was regularly replaced every 2 h (except overnight) to remove the surfactant mixture.[13]

Characterization. Before electrodeposition, the phase behavior of the electrolyte mixture was investigated using a Nikon Microphot-FXA microscope at room temperature and by low-angle X-ray diffraction (XRD). Thin films of the liquid crystals were prepared by sandwiching the mixture between a glass microscope slide and coverslip and cooling from 50 to 60 °C to room temperature for microscopy. The liquid crystal electrolyte was just put in the powder XRD sample holder for XRD because such an electrolyte is very viscous at room temperature. XRD patterns were recorded on a Siemens D-500 diffractometer using Cu Kα radiation. Scanning electron microscopy (SEM) images were obtained in a Philips XL30-FEG operated at 20 kV. Transmission electron microscopy (TEM) images and electron diffraction (ED) patterns were obtained on a Philips CM300 equipped with energy-dispersive X-ray (EDX) spectrometer and operated at 120 kV. The samples for TEM were prepared by scraping off films from Au−Si or ITO glass directly onto carbon-coated copper grid. Magnetic hysteresis loops were measured using a vibrating sample magnetometer (VSM) at room temperature.

Results and Discussion

Electrodeposition of Mesoporous Bi Film. a. Electrochemical Studies. The cyclic voltamogram (CV) of film deposition from 50 wt % Brij76 templated Bi electrolyte (Figure 1b) at a scan rate of 10 mV/s over the potential range +0.5 to −1 V is similar to that of deposition from Bi electrolyte without surfactant (Figure 1a). The sweep starts at open-circuit potential about +0.3 V. The current−voltage curves exhibit a characteristic reduction peak due to the diffusion-limited deposition of Bi with the peak at around −0.3 V. On the reverse scan a large stripping peak of Bi is observed. It is noted that the current−voltage curve from electrolytes containing Brij56 is the same as Brij76. The deposition of mesoporous Bi film has quite lower current densities than the deposition of the nonporous film. Based on the CV curves, the nonporous Bi and mesoporous Bi films were carried out potentiostatically at −0.3 V vs Ag/AgCl, and the film thickness could be easily controlled by the charge according to Faraday's law if the current efficiency of 100% was assumed. The thickness of all films was controlled to be 1 μm, and the thickness was also measured by a Dektak-3 surface profiler. Note that the electrodeposited film surface is not perfectly smooth.

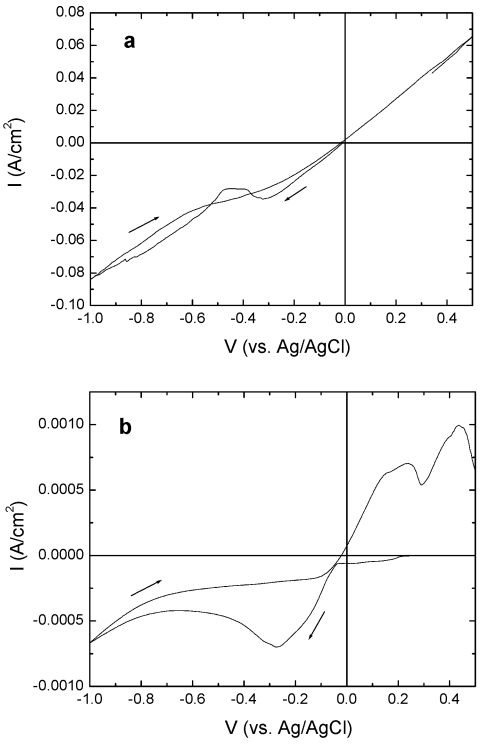

Figure 1. Cyclic voltammogram (CV) of film deposition on Au from Bi electrolyte (a) and from 50 wt % Brij76 templated Bi electrolyte (b).

b. Structural Analysis. Metals (e.g., Pt, Pd, Sn, Ni, Co) or elemental semiconductors (e.g., Se, Te) with well-defined periodic hexagonal mesopores have been electrodeposited from lyotropic liquid crystalline phases of nonionic surfactants.[11−20] Since the nanostructured films are a direct cast of the structure of the lyotropic liquid crystalline phases used to template the deposition, it is important to investigate the phase structure of the electrolyte before electrodeposition. The electrolyte mixture phase structures were examined by low-angle X-ray diffraction (XRD) (Figure 2a). The Brij76 templated Bi electrolyte shows four peaks with d spacing of 7.0, 3.6, 2.4, and 1.8 nm (ratio is 1:2:3:4), which can be indexed as (001), (002), (003), and (004) reflections associated with the lamellar symmetry. Brij56 templated Bi electrolyte also shows lamellar structure with four well-resolved peaks with d spacing of 5.9, 3, 2, and 1.5 nm.

Low-angle XRD patterns for the corresponding mesoporous Bi films are shown in Figure 2b. Brij76 templated porous Bi film has one broad peak with fwhm (full width half-maximum) of 0.8°, and Brij56 templated Bi film has one broad peak with fwhm of 0.6°. Low-angle diffraction peaks were not observed for nonporous films deposited in the absence of surfactants (not shown here). The appearance of low-angle peaks indicates the presence of meso-

(26) Whitney, T. M.; Jiang, J. S.; Searson, P. C.; Chien, C. L. *Science* **1993**, *261*, 1316.

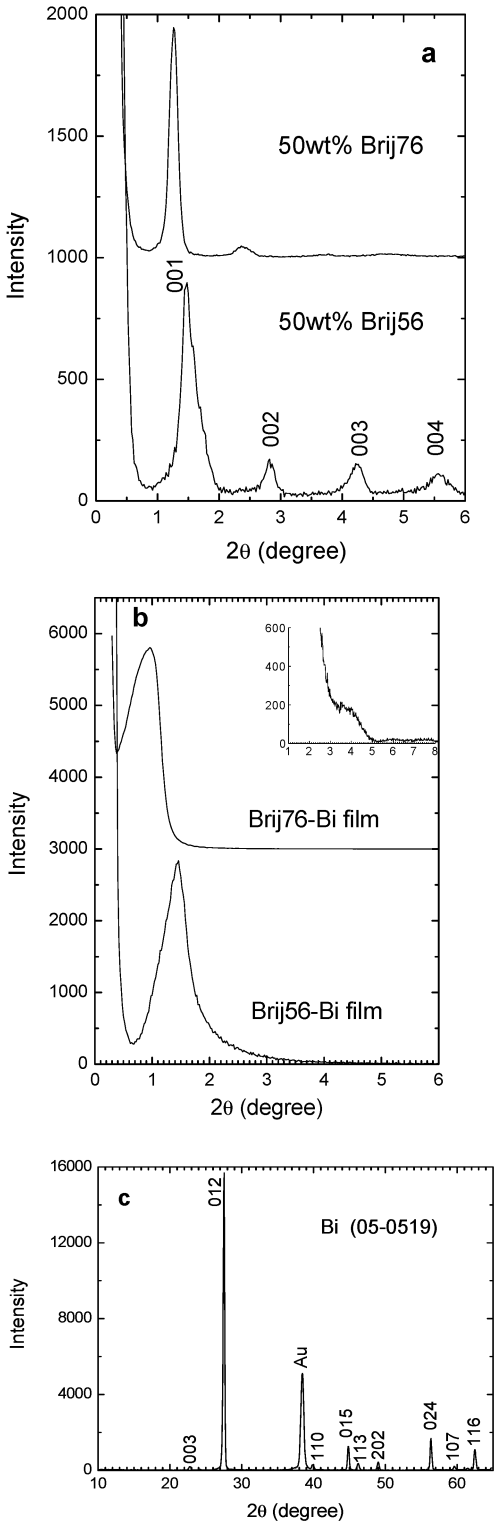

Figure 2. (a) Low-angle XRD patterns for Brij56 and Brij76 templated Bi electrolyte, (b) low-angle XRD patterns for mesoporous Brij56 and Brij76−Bi films, and (c) wide-angle XRD pattern for mesoporous Brij76−Bi film grown on Au−Si.

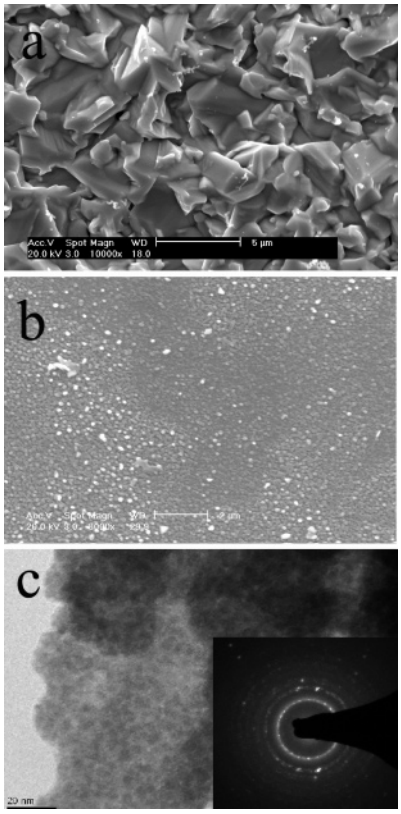

Figure 3. SEM images of Bi films on Au: (a) nonporous Bi film, (b) mesoporous Brij76−Bi film, and (c) TEM image of mesoporous Brij76−Bi film. The inset is the electron diffraction (SAED) pattern.

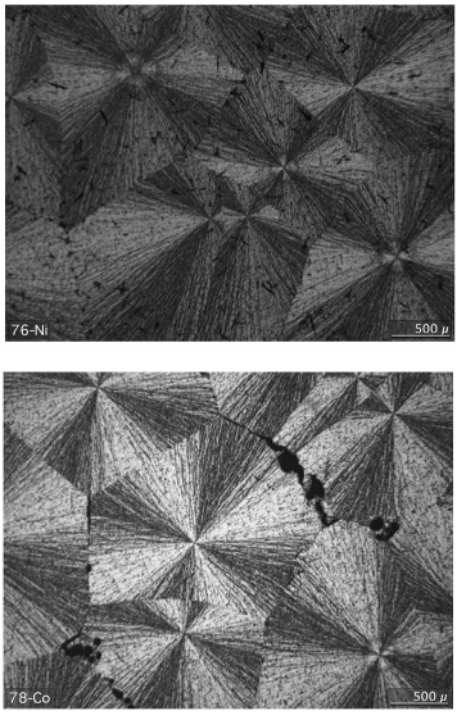

Figure 4. Polarized-light optical microscopy (POM) images for Brij76 templated Ni electrolyte from $NiAc_2$ (a, top) and Brij78 templated Co electrolyte from $CoAc_2$ (b, bottom).

pores in the Bi film. However, only one peak in the low-angle range indicates that the ordering is limited. The templates for the deposition of metal films in Figure 2a clearly have lamellar structures. It has been generally observed that mesoporous materials could be a direct cast of the structure of the lyotropic liquid crystalline templates.[11−20] Thus, we expected that the Bi film would have lamellar mesostructure. However, the low-angle XRD patterns seem to suggest that the lamellar structures have partially collapsed, leading to disordered porous films after electrodeposition and surfactant removal, and this is consistent with TEM image (Figure 3c). Figure 2b shows

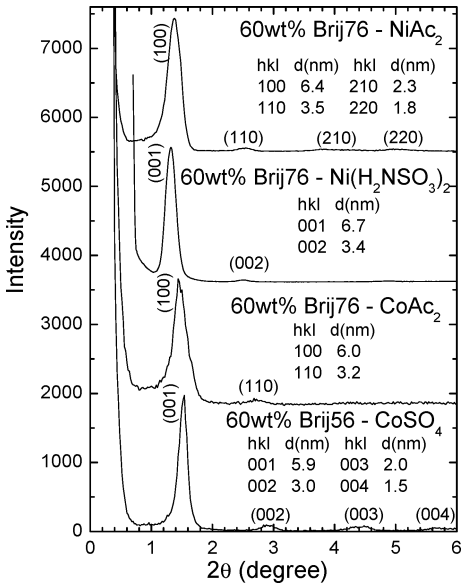

Figure 5. Low-angle XRD patterns for Brij56 or Brij76 templated Ni and Co electrolytes.

that Brij76 templated porous Bi film has a *d* spacing of 7.8 nm and Brij56 templated Bi film has 5.8 nm, which are consistent with the relative template sizes. It is known that the size of pores can be varied by using surfactants of different alkyl chain length in the lyotropic liquid crystalline phases.[11−20] As expected, the use of larger surfactant molecule Brij76 caused an increase in the *d* spacing of the resulting mesostructure as compared with Brij56 templated mesoporous films. The wide-angle XRD patterns for nonporous and mesoporous Bi films are similar, and the Brij76 templated mesoporous Bi film is shown in Figure 2c. Except for the substrate Au peaks, all other peaks belong to rhomhedral Bi structure (JCPDS, no. 05-0519) without any impurity.

c. Film Microstructure. The surface morphology of nonporous and mesoporous Bi films has been investigated by scanning electron microscopy (SEM), and their images are shown in Figure 3a,b. The mesoporous Bi film has clearly smaller particle size than the nonporous film. The transmission electron microscopy (TEM) image (Figure 3c) does not show a highly ordered pore structure, which is consistent with only one peak appearing in low-angle XRD pattern (Figure 2b). It reveals mesoporous structure with about 3 nm pore size. The pore diameter is comparable with that found from TEM for mesoporous Pt, Ni, Se, and Te films electrodeposited from the liquid crystal phases of the same surfactant Brij56 or Brij76.[11−20] The dark regions correspond to the pores left after surfactant removal whereas the light regions correspond to the deposited Bi. The selected area electron diffraction (SAED) (inset in Figure 3c) confirms the pure crystalline Bi formation. Usually for mesostructured silica, lamellar structure easily collapses upon calcination to remove surfactant.[27] However, very recently, lamellar mesostructured ZnO and WO_3 films were fabricated by electrodeposition utilizing potential-controlled self-assembly of surfactant−inorganic aggregates at the solid−liquid interface, and the structure was stable after the surfactant SDS was removed by washing film with water and ethanol.[28,29] This and our result may imply one of the unique features of electrochemical method.

Electrodeposition of Mesoporous Ni and Co Films. a. Structural Analysis. Before electrodeposition, polarized-light optical microscopy (POM) and low-angle XRD were used to determine the electrolyte phase structure. Figure 4 show the typical POM images for Brij76 or Brij78 templated Ni and Co electrolytes. The equal 120° spacing between the three axes in the same plane is a clear indication of the hexagonal structure.[25] Figure 5 shows the low-angle XRD patterns. The Brij76 templated Ni electrolytes from $NiAc_2$ show four well-resolved peaks with *d* spacing of 6.4, 3.5, 2.3, and 1.8 nm, which can be indexed as (100), (110), (210), and (220) reflections associated with the 2D hexagonal symmetry. For the Brij76 templated Co electrolyte from $CoAc_2$, it also shows hexagonal symmetry with *d* spacing of 6.0 and 3.2 nm for (100) and (110) reflections. But for electrolyte from $CoSO_4$, it shows lamellar structure with four well-resolved peaks of *d* spacing of 5.9, 3, 2, and 1.5 nm. Similarly, the electrolyte from $Ni(H_2NSO_3)_2$ also shows lamellar structure with *d* spacing of 6.7 and 3.4 for (001) and (002) reflections. It

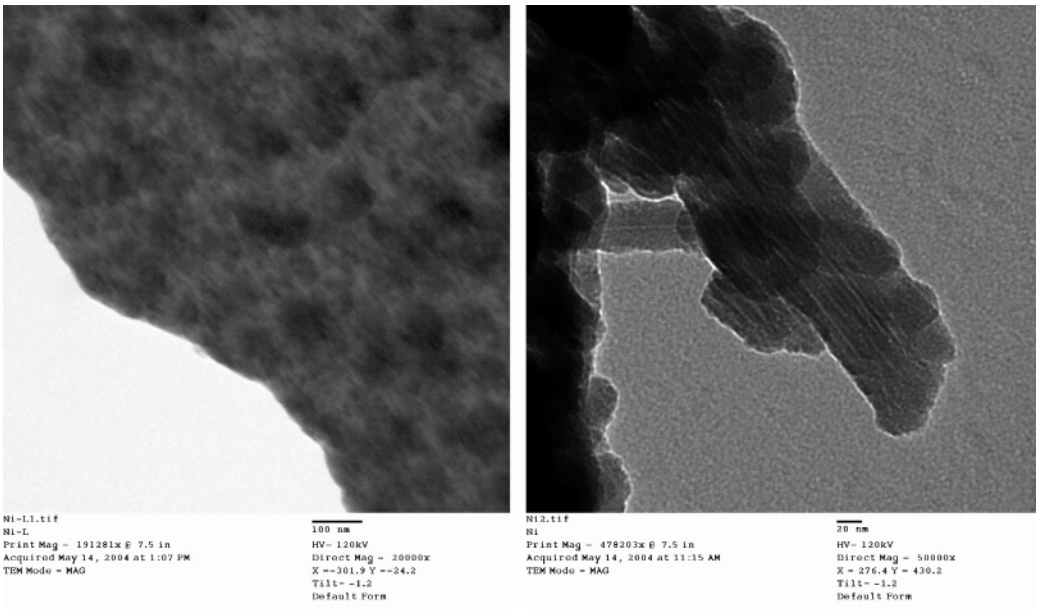

Figure 6. TEM images for (left) lamellar mesostructured Ni film from Brij76-$Ni(H_2NSO_3)_2$, and (right) hexagonal Ni film from Brij76-$NiAc_2$.

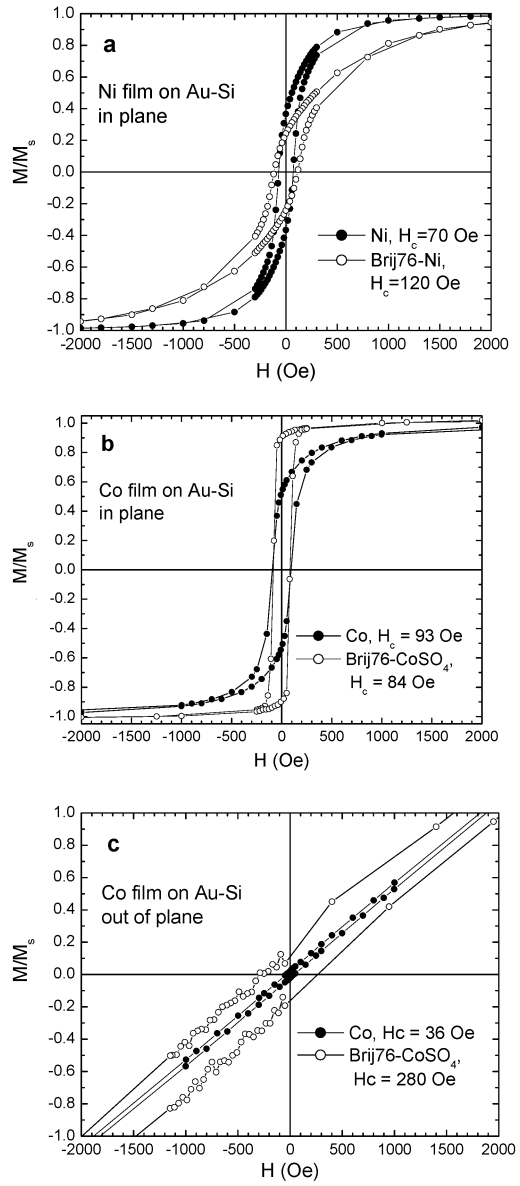

Figure 7. Normalized magnetization curves measured at room temperature for Ni and Co films: (a) nonporous polycrystalline Ni film and mesoporous Brij76−Ni film with hexagonal structure, magnetic field applied parallel to the film; (b) nonporous polycrystalline Co film and mesoporous Brij76−Co film with lamellar structure, magnetic field applied parallel to the film; and (c) nonporous polycrystalline Co film and mesoporous Brij76−Co film with lamellar structure, magnetic field applied perpendicular to the film.

appears that, using different chemical precursors, the mesoporous structure (e.g., hexagonal or lamellar) of the Ni and Co template electrolytes can be easily controlled. It is also noted that using different surfactant such as Brij56, Brij76, or Brij78 with the same electrolyte composition resulted in the same structure in the final films. Very recently, Dag et al. investigated the interaction between some metal complex salts $[M(H_2O)_x]Y_2$ (where $M = Co^{2+}, Ni^{2+}, Zn^{2+}, Cr^{3+}$, $Y = Cl^-, NO_3^-, ClO_4^-$) and nonionic surfactants (such as $C_{12}EO_{10}$) and found that the anions have a greater influence on the hydrophilicity of surfactants than do cations. The self-assembly of hexagonal and cubic mesostructures can be controlled by the hydrophilicity of the nonionic surfactant through choosing the right anion type of the metal salts.[30] Similarly, our results show that hexagonal mesostructures can be obtained by self-assembly of nonionic surfactant and $Ni(Ac)_2$ or $Co(Ac)_2$, and lamellar structure can be obtained in $CoSO_4$ or $Ni(H_2NSO_3)_2$. Figure 6 shows TEM images for mesoporous Ni films from Brij76 lamellar liquid crystal phase from $Ni(H_2NSO_3)_2$ and hexagonal liquid crystal phase from $NiAc_2$, respectively. The mesoporosity of hexagonal Ni is well-ordered, and channels have long-range continuity. The observed parallel lines have a repeat distance of 3 nm, suggesting hexagonally close-packed cylindrical pores with a uniform pore diameter of 3 nm, and this is consistent with previous observations of hexagonally oriented channels of other mesoporous materials prepared by electrodeposition.[16,17,25] However, for lamellar liquid crystal templated Ni, similar to lamellar Bi, it does show porosity, but it is difficult to see the highly ordered pore arrangement. EDX analyses on thick pieces sample indicate that there is little amount of carbon, which verifies that most of the surfactant was removed by water extraction.

b. Magnetic Properties. We carried out preliminary studies of the magnetic properties for the nanostructured mesoporous magnetic films. Figure 7 shows the magnetic hysteresis loops for mesoporous Ni and Co films on Au−Si at room temperature compared with nonporous films. It is clear that the there is an increase in the coercivity, H_c, from 70 Oe for the nonporous polycrystalline Ni film to 120 Oe for mesoporous Ni film with hexagonal structure, when the magnetic field is parallel to the films. For mesoporous Co film with hexagonal structure, similar to Ni, an increase of coercivity was observed. But for mesoporous Co film with lamellar structure, the in-plane coercivity was slightly decreased from 93 Oe of the nonporous polycrystalline Co film to 84 Oe for the porous film. However, the out-of-plane coercivity was increased dramatically from 36 to 280 Oe. It is noted that magnetic properties of metal films are strongly influenced by texture. The grain structure and morphology of the dense film and mesoporous films are significantly different. In addition, magnetic properties including the coercivity also change with the pore diameter. Therefore, further study is needed to provide more definitive conclusions.

Acknowledgment. We thank Dr. K. N. Bozhilov for TEM images. We acknowledge the financial support from Riverside Public Utilities, California Energy Commission, and UC-SMART.

LA036367+

(27) Edler, K. J.; Roser, S. J. *Int. Rev. Phys. Chem.* **2001**, *20*, 387.
(28) Choi, K.-S.; Lichtenegger, H. C.; Stucky, G. C. *J. Am. Chem. Soc.* **2002**, *124*, 12402.
(29) Baeck, S.-H.; Choi, K.-S.; Jaramillo, T. F.; Stucky, G. D.; McFarland, E. W. *Adv. Mater.* **2003**, *15*, 1269.
(30) Dag, Ö; Alayoğlu, S.; Uysal, İ. *J. Phys. Chem. B* **2004**, *108*, 8439.